Analysis of heavily boron-doped diamond Raman spectrum

V. Mortet[a,b] , A. Taylor[a], Z. Vlčková Živcová[c], D. Machon[d], O. Frank[c], P. Hubík[e], D. Tremouilles[f], L. Kavan[c]

[a] Institute of Physics of the Czech Academy of Sciences, Na Slovance 1999/2, 182 21, Prague 8, Czech Republic

[b] Czech Technical University in Prague, Faculty of Biomedical Engineering, Sítna 3105, 272 01, Kladno, Czech Republic

[c] J. Heyrovsky Institute of Physical Chemistry of the Czech Academy of Sciences, Dolejskova 3, 182 23, Prague 8, Czech Republic

[d] Université de Lyon, F-69000 Lyon, France and Institut Lumière Matière, CNRS, UMR 5306, Université Lyon 1, F-69622 Villeurbanne, France

[e] Institute of Physics of the Czech Academy of Sciences, Cukrovarnicka 10, 162 00, Prague 6, Czech Republic

[f] LAAS-CNRS, Université de Toulouse, 7, avenue du Colonel Roche, 31031, Toulouse Cedex 4, France

Lattice disorder, electronic Raman scattering, and Fano interaction effects are at the genesis of the Raman spectrum of heavily boron-doped diamond. However, no accurate unified description of this spectrum has been reported yet. In this work, we propose novel analysis of the Raman spectrum of boron-doped diamond based on classical models of electronic Raman scattering and Fano effect. This new analysis shows that the Raman spectrum of boron-doped diamond results from the combination of electronic Raman scattering and its interaction, i.e. Fano effect, with the diamond phonon density of states and it confirms the 500 cm^{-1} and 1200 cm^{-1} bands originate from the phonon density of states.

Introduction

Raman spectroscopy is a fast and nondestructive technique widely used for the characterization of diamonds. Intensities, position and full width at half maximum of Raman peaks are representative of the quality and composition of diamond layers. For instance, heavily boron-doped diamond with metallic electrical conductivity has a characteristic Raman signature with two broad bands at ca. 500 cm^{-1} (B1) and ca. 1200 cm^{-1} (B2) along with a Fano-shaped zone-center phonon (ZCP) peak below 1332 cm^{-1}. It is conjectured the Fano-shape results from interaction between discrete diamond zone-center phonon (ZCP) and electronic Raman scattering effects. The majority of studies on the Fano-shaped diamond peak reports a negative value for the Fano asymmetric parameter (q) [1-7]. Other authors reported positive values of the Fano asymmetric parameter in layers [2,8,9] with boron concentrations close to the metal-insulator transition (Mott transition). The origin of other Raman peaks is subject to discussion. The B2 band had previously been attributed to vibration modes of boron atoms [10]. However, substitutional isotopic studies have, unambiguously, demonstrated its vibration origin to be related to carbon atoms [1,11,12]. It is generally agreed that this band corresponds to a maximum of the diamond phonon density of states (PDoS) [13,14] . The appearance of this Raman forbidden band is due to the relaxation of the Raman wave vector conservation rule in materials with high lattice disorder [7,15], i.e., the high

concentration of substitutional boron atoms in the diamond lattice. However, this interpretation is not fully satisfactory due to the mismatch between the experimental peak position , the known optical maxima of diamond's PDoS [16] and contradictory reports of the peak shape: Szirmai et al. presented this peak as symmetrical with a Lorentzian shape [1], whereas Bustarret et al. depicted it as an asymmetric Fano-shaped peak [3,17]. The broad asymmetric band B1 is empirically modeled with the sum of a Lorentzian and a Gaussian [18] or a Lorentzian component [1]. It is very sensitive to the boron concentration [19,20] and it was attributed to vibration modes of boron dimers [18,21]. However, substitutional isotopic studies have failed to unambiguously confirm this assignment [12, 14]. The purpose of this article is to address these contradictions. Based on classic models of electronic Raman scattering, Fano effect, and analytical methodology we clarify the origin of the Raman spectrum of the boron-doped diamond.

Experimental

In order to remove any added complication due to the presence of sp^2 carbon phase Raman features, which are present in polycrystalline diamond layers, this study has been carried out on epitaxial boron-doped diamond layers. The studied epitaxial layers were grown on high pressure and high-temperature diamond substrates in a 1.5 kW resonance cavity microwave plasma enhanced chemical vapor deposition system, AX5010 from Seki Diamond Systems, with two different boron concentrations. Sample S1 was grown with a boron to carbon ratio, in the gas phase, of 4,000 ppm on a (100) oriented substrate using deposition conditions reported in ref. [22], whereas sample S2 was grown with a higher boron to carbon ratio of 40,000 ppm on a (111) oriented substrate using deposition conditions reported in ref. [20]. Raman spectra were measured using a LabrRAM HR spectrometer from Horiba Jobin-Yvon interfaced to an Olympus microscope with a 100× objective and a 50 µm confocal aperture, and a HeNe laser 633 nm (1.96 eV) with 8 mW power. The spectrometer was calibrated using the silicon F_{1g} peak at 520.2 cm^{-1} and its spectral response was calibrated using a certified HL-2000 Tungsten Halogen Light Source from Ocean Optics. Raw Raman spectra were corrected for instrumental response, temperature effect and the frequency factor [23-25]. The temperature correction is particularly important in order to observe the broad electronic Raman scattering response. Corrected spectra or reduced Raman ($I_r(\omega)$) spectra are calculated using equation (1) with $I(\omega)$ the experimental spectrum, $K(\omega)$ the spectrometer response; ω_L the absolute frequency of laser excitation line, ω the Raman shift, and $n(\omega)$+1 the thermal population factor with $n(\omega$, T) the Bose-Einstein distribution.

$$I_r(\omega) = I(\omega).[K(\omega).(\omega_L - \omega)^4.\omega^{-1}.(n(\omega,T)+1)]^{-1} \qquad \text{(eq. 1)}$$

Results and discussion

Normalized raw and reduced Raman spectrum of both samples are shown in figure 1 and figure 2, respectively. The raw spectra are characteristic of boron-doped diamond with metallic electrical conductivity with low (sample S1) and high boron concentration (sample S2) [17,19]. In contrary to sample S2, sample S1 exhibits no measurable band at ca. 500 cm^{-1}. Both reduced spectra retain the characteristic band of boron-doped diamond. They share a broad asymmetric background with a maximum between 1000 and 2000 cm^{-1} attributed to electronic Raman scattering, a broadband B2 merged with the narrow diamond line, and a broad dip at 1350 cm^{-1} attributed to Fano antiresonance. The large width of this dip cannot originate only from the antiresonance of the Fano shaped narrow diamond line. We attribute this dip to a combination of the Fano antiresonance of the B2 band and the diamond line. This assumption is

supported by the clear asymmetry of the B2 band, which is characteristic for Fano effect, and is consistent with the work of Bustarret et al. [3]. The two Raman spectra exhibit a different curvature at low wavenumbers, i.e., < 500 cm^{-1}. The concavity of S1 spectrum is consistent with electronic Raman scattering whereas the convexity of S2 sample may be attributed to a Fano antiresonance of the B1 band. This assumption is supported by the well-known asymmetry of this band. Based on these observations, we constructed a fitting function to describe the Raman spectrum of boron-doped diamond assuming the interaction of the observed Raman lines with electronic Raman scattering applies to the diamond ZCP phonon line and all other observed bands using well-established model of electronic Raman scattering and Fano effect. This hypothesis is legitimized by the asymmetric nature of the different bands and the broad range of electronic Raman scattering.

To our knowledge and in contrary to metals [26,27] and heavily doped silicon [28], electronic Raman scattering has not been investigated in boron-doped diamond. In this work, the normalized electronic Raman scattering $I_e(\omega)$ is modelled using the equation (2) used for Raman scattering by intra-band excitations and where ω_e is the position of the maximum of the electronic Raman scattering spectrum. This equation was shown to satisfactorily describe electronic Raman scattering in conventional elemental metals [27] and highly doped semiconductors [29].

$$I_e(\omega) = \frac{2.(\omega/\omega_e)}{1+(\omega/\omega_e)^2} \qquad \text{(eq. 2)}$$

Fano shaped peaks are modeled using the normalized Fano function $F_j(\omega)$ (see equations 3 and 4) with q_j the Fano asymmetric parameter, ω_j the center position and Γ_j the full width at half maximum of the Lorentzian shaped Raman lines.

$$F_j(\omega) = \frac{1}{1+q_j^2}\frac{(q_j+\varepsilon_j)^2}{1+\varepsilon_j^2} \qquad \text{(eq. 3)}$$

$$\text{with} \quad \varepsilon_j(\omega) = \frac{\omega-\omega_j}{\Gamma_j} \qquad \text{(eq. 4)}$$

Based on the assumptions above, the reduced Raman spectrum of boron-doped diamond is fitted using equation (5) representing the sum of the different weighted light scattering events: pure electronic Raman scattering and its interaction with the different localized Raman scatterings. A_e is the weighted factor of pure electronic Raman scattering and A_j are the weighting factor of the different Fano-shaped peaks.

$$I_r(\omega) = I_e(\omega).\left[A_e + \sum_j A_j.F_j(\omega)\right] \quad \text{(eq. 5)}$$

The Raman spectra of diamond samples were fitted with equation (5) using the non-linear fitting tool of Origin 2016 © software. The fitting function and its different components are reported in figure 2, and the fitting parameter is reported in Table I. The fitting function satisfactorily models the B2 band, the diamond lines, and antiresonance dip as well as the broad B1 band. It particularly shows that the broad antiresonance dip at ca. 1350 cm^{-1} is a combination of the diamond ZCP and the B2 bands antiresonances. The Fano asymmetric parameter values of the B2 band are remarkably close to the ones of the ZCP line, which are consistent with values reported in the literature [1–6] and the position and the width of the diamond line are also consistent with our previous report [20]. The fitting peak position of the B2 band (1250 cm^{-1}) corresponds to the reported maxima of diamond PDoS [16] which supports our analysis and confirms the PDoS origin of this band. Similarly, the fitting peak position (427 cm^{-1}) and width (90 cm^{-1}) of

the B1 band are comparable with the reported values of the acoustic maximum of PDoS peak measured by Raman spectroscopy on not electrically conductive diamond nanoparticles and disordered diamond [30,31]. The assignment of the B1 band to a maximum of the acoustic branch of the PDoS is consistent with was already hypothesized by several other authors [7,32]. This analysis indicates that the difference between the apparent position of the B1 band and the position of the maximum of PDoS in disordered diamond is not only due to phonon confinement but it is also due its interaction with electronic Raman scattering, i.e. Fano effect, conformably with the ZCP line [20]. This analysis is also analogous to Yogi et al. work on silicon nanostructures who report the observation of a size-dependent position asymmetric peak due to acoustic phonons by Raman spectroscopy due to the quantum confinement effect and their interaction with intraband quasi-continuum [33].

Conclusion

In summary, we have shown the total Raman spectrum of highly boron-doped diamond can be satisfactorily fitted using the combination of well-established electronic Raman scattering and Fano effect models. This analysis shows that not only the diamond ZCP band is Fano-shaped but also the 500 cm^{-1} and 1200 cm^{-1} bands. As a result, their apparent position is shifted from their normal position, which corresponds to the acoustic and optical maxima of the phonon density of states in disordered diamond.

Acknowledgment: This work was financially supported by project 13-31783S of Czech Science Foundation, the French-Czech Project Barrande 35785SC - 7AMB16FR004 of the Czech Ministry of Education, Youth and Sports and the J.E. Purkyně fellowship awarded to V. Mortet by the Czech Academy of Sciences.

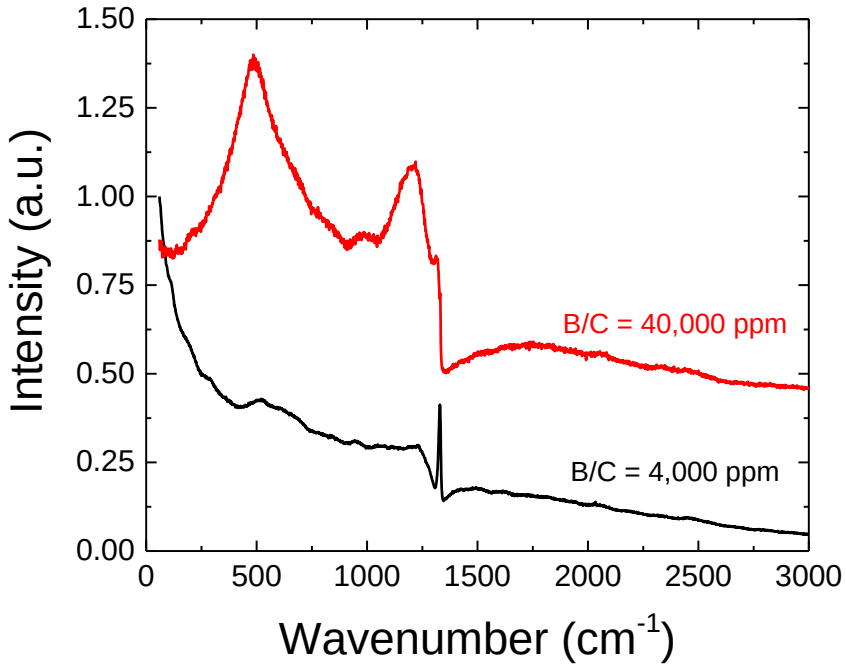

Fig. 1: Normalized raw Raman spectra of boron-doped diamond samples grown at B/C ratios of 4,000 ppm (S1) and 40,000 ppm (S2). The spectra of sample S2 is shifted by + 0.4 units for improved readability.

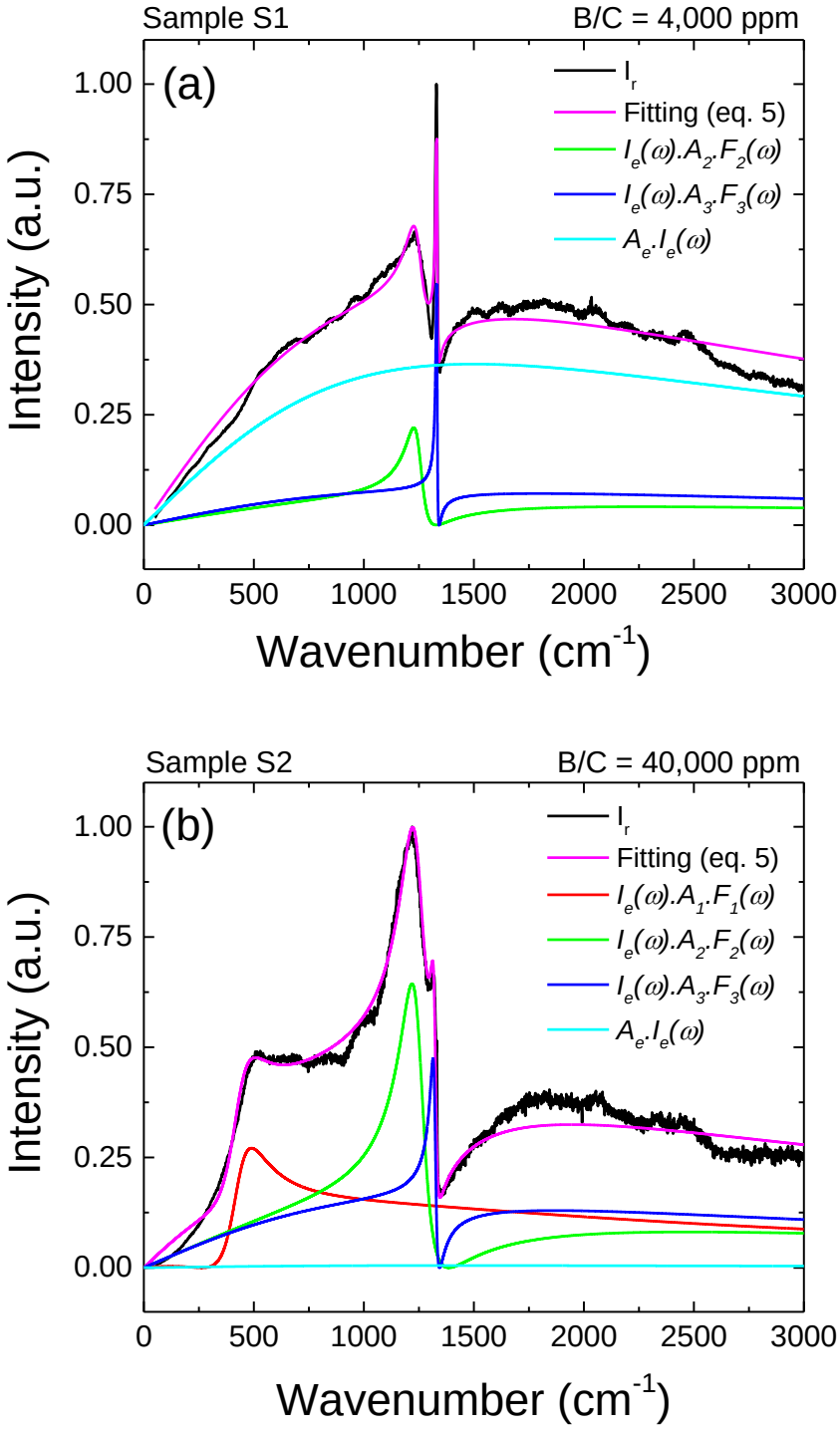

Fig. 2. Experimental reduced and normalized Raman spectra (solid black line) of boron-doped diamond samples grown at B/C ratios of 4,000 ppm (S1) and 40,000 ppm (S2) , mathematical fittings (magenta solid line) with the contribution of the different Fano shape peaks (red, green and blue lines) and pure electronic Raman scattering broadband (cyan solid line).

Table I Fitting parameter values of boron-doped diamond layer Raman spectra. Indices 1, 2, and 3 correspond to the B1 band, B2 band, and ZCP line, respectively.

Parameter	**Sample S1 (B/C = 4,000 ppm)**	**Sample S2 (B/C = 40,000 ppm)**
ω_e	1400	1400
A_e	0.365	0.005
A_1	-	0.88
q_1	-	1.83
ω_1	-	427.2
Γ_1	-	90
A_2	0.45	1.3
q_2	-1.75	-2.1
ω_2	1250.9	1249.5
Γ_2	40.7	65
A_3	1.1	0.95
q_3	-2.5	-1.5
ω_3	1332	1323.3
Γ_3	4.3	13.9

References

[1] P. Szirmai, T. Pichler, O.A. Williams, S. Mandal, C. Bäuerle, F. Simon, A detailed analysis of the Raman spectra in superconducting boron doped nanocrystalline diamond, Physica Status Solidi (B). 249 (2012) 2656–2659. doi:10.1002/pssb.201200461.

[2] K. Ushizawa, K. Watanabe, T. Ando, I. Sakaguchi, M. Nishitani-Gamo, Y. Sato, H. Kanda, Boron concentration dependence of Raman spectra on {100} and {111} facets of B-doped CVD diamond, Diamond and Related Materials. 7 (1998) 1719–1722.

[3] E. Bustarret, E. Gheeraert, K. Watanabe, Optical and electronic properties of heavily boron-doped homo-epitaxial diamond, Physica Status Solidi (A). 199 (2003) 9–18. doi:10.1002/pssa.200303819.

[4] F. Pruvost, A. Deneuville, Analysis of the Fano in diamond, Diamond and Related Materials. 10 (2001) 531–535. doi:10.1016/S0925-9635(00)00378-2.

[5] C. Piccirillo, A. Mainwood, G. Davies, C.M. Penchina, A. Tajani, M. Bernard, A. Deneuville, The Temperature Dependence of the Infrared Absorption and Raman Spectra Due to Boron in Diamond, Physica Status Solidi (A). 193 (2002) 529–534. doi:10.1002/1521-396X(200210)193:3<529::AID-PSSA529>3.0.CO;2-5.

[6] P. Gonon, E. Gheeraert, A. Deneuville, F. Fontaine, L. Abello, G. Lucazeau, Characterization of heavily B-doped polycrystalline diamond films using Raman spectroscopy and electron spin resonance, Journal of Applied Physics. 78 (1995) 7059–7062. doi:10.1063/1.360410.

[7] E. Gheeraert, P. Gonon, A. Deneuville, L. Abello, G. Lucazeau, Effect of boron incorporation on the “quality” of MPCVD diamond films, Diamond and Related Materials. 2 (1993) 742–745. doi:10.1016/0925-9635(93)90215-N.

[8] R. Locher, J. Wagner, F. Fuchs, M. Maier, P. Gonon, P. Koidl, Optical and electrical characterization of boron-doped diamond films, Diamond and Related Materials. 4 (1995) 678–683.

[9] A.N. Utyuzh, Y.A. Timofeev, A.V. Rakhmanina, Effect of boron impurity on the Raman spectrum of synthetic diamond, Inorganic Materials. 40 (2004) 926–931.

[10] M. Werner, O. Dorsch, H.U. Baerwind, E. Obermeier, L. Haase, W. Seifert, A. Ringhandt, C. Johnston, S. Romani, H. Bishop, P.R. Chalker, Charge transport in heavily B-doped polycrystalline diamond films, Applied Physics Letters. 64 (1994) 595–597. doi:10.1063/1.111088.

[11] N. Dubrovinskaia, L. Dubrovinsky, T. Papageorgiou, A. Bosak, M. Krisch, H.F. Braun, J. Wosnitza, Large carbon-isotope shift of TC in boron-doped diamond, Applied Physics Letters. 92 (2008) 132506. doi:10.1063/1.2906381.

[12] P. Achatz, F. Omnès, L. Ortéga, C. Marcenat, J. Vacík, V. Hnatowicz, U. Köster, F. Jomard, E. Bustarret, Isotopic substitution of boron and carbon in superconducting diamond epilayers grown by MPCVD, Diamond and Related Materials. 19 (2010) 814–817. doi:10.1016/j.diamond.2010.01.052.

[13] V.A. Sidorov, E.A. Ekimov, Superconductivity in diamond, Diamond and Related Materials. 19 (2010) 351–357. doi:10.1016/j.diamond.2009.12.002.

[14] I.I. Vlasov, E.A. Ekimov, A.A. Basov, E. Goovaerts, A.V. Zoteev, On the origin of the Raman scattering in heavily boron-doped diamond, ArXiv Preprint ArXiv:0801.1611. (2008). https://arxiv.org/abs/0801.1611.

[15] K.K. Tiong, P.M. Amirtharaj, F.H. Pollak, D.E. Aspnes, Effects of As+ ion implantation on the Raman spectra of GaAs: “Spatial correlation” interpretation, Applied Physics Letters. 44 (1984) 122–124. doi:10.1063/1.94541.

[16] A.M. Zaitsev, Optical properties of diamond: a data handbook, Springer Science & Business Media, 2013.

[17] S. Ghodbane, A. Deneuville, Specific features of 325 nm Raman excitation of heavily boron doped polycrystalline diamond films, Diamond and Related Materials. 15 (2006) 589–592. doi:10.1016/j.diamond.2005.12.054.

[18] M. Bernard, C. Baron, A. Deneuville, About the origin of the low wave number structures of the Raman spectra of heavily boron doped diamond films, Diamond and Related Materials. 13 (2004) 896–899. doi:10.1016/j.diamond.2003.11.082.
[19] M. Bernard, A. Deneuville, P. Muret, Non-destructive determination of the boron concentration of heavily doped metallic diamond thin films from Raman spectroscopy, Diamond and Related Materials. 13 (2004) 282–286. doi:10.1016/j.diamond.2003.10.051.
[20] V. Mortet, Z. Vlčková Živcová, A. Taylor, O. Frank, P. Hubík, D. Trémouilles, F. Jomard, J. Barjon, L. Kavan, Insight into boron-doped diamond Raman spectra characteristic features, Carbon. 115 (2017) 279–284. doi:10.1016/j.carbon.2017.01.022.
[21] E. Bourgeois, E. Bustarret, P. Achatz, F. Omnès, X. Blase, Impurity dimers in superconducting B-doped diamond: Experiment and first-principles calculations, Physical Review B. 74 (2006). doi:10.1103/PhysRevB.74.094509.
[22] V. Mortet, L. Fekete, P. Ashcheulov, A. Taylor, P. Hubík, D. Tremouilles, E. Bedel-Pereira, (100) Substrate processing optimization for fabrication of smooth boron doped epitaxial diamond layer by PE CVD, Proceedings of NANOCON 2014, 6th International Conference, 2014, Brno, Czech Republic, EU, November 5-7th, 2014. (2015) 115–119.
[23] R. Carles, M. Bayle, P. Benzo, G. Benassayag, C. Bonafos, G. Cacciato, V. Privitera, Plasmon-resonant Raman spectroscopy in metallic nanoparticles: Surface-enhanced scattering by electronic excitations, Physical Review B. 92 (2015). doi:10.1103/PhysRevB.92.174302.
[24] M.H. Brooker, O.F. Nielsen, E. Praestgaard, Assessment of correction procedures for reduction of Raman spectra, Journal of Raman Spectroscopy. 19 (1988) 71–78.
[25] R. Shuker, R.W. Gammon, Raman-Scattering Selection-Rule Breaking and the Density of States in Amorphous Materials, Physical Review Letters. 25 (1970) 222–225. doi:10.1103/PhysRevLett.25.222.
[26] W. Akemann, A. Otto, Electronic Raman scattering at disordered noble- and alkali-metal surfaces, Philosophical Magazine B. 70 (1994) 747–760. doi:10.1080/01418639408240247.
[27] Y.S. Ponosov, S.V. Streltsov, Measurements of Raman scattering by electrons in metals: The effects of electron-phonon coupling, Physical Review B. 86 (2012). doi:10.1103/PhysRevB.86.045138.
[28] I.P. Ipatova, A.V. Subashiev, V.A. Voitenko, Electron light scattering from doped silicon, Solid State Commun. 37 (1981) 893.
[29] G. Contreras, A.K. Sood, M. Cardona, Raman scattering by intervalley carrier-density fluctuations in n-type Si: Intervalley and intravalley mechanisms, Physical Review B. 32 (1985) 924.
[30] S. Prawer, K.W. Nugent, D.N. Jamieson, J.O. Orwa, L.A. Bursill, J.L. Peng, The Raman spectrum of nanocrystalline diamond, Chemical Physics Letters. 332 (2000) 93–97.
[31] J.O. Orwa, K.W. Nugent, D.N. Jamieson, S. Prawer, Raman investigation of damage caused by deep ion implantation in diamond, Physical Review B. 62 (2000) 5461.
[32] S. Prawer, R.J. Nemanich, Raman spectroscopy of diamond and doped diamond, Philosophical Transactions of the Royal Society A: Mathematical, Physical and Engineering Sciences. 362 (2004) 2537–2565. doi:10.1098/rsta.2004.1451.
[33] P. Yogi, S. Mishra, S.K. Saxena, V. Kumar, R. Kumar, Fano Scattering: Manifestation of Acoustic Phonons at the Nanoscale, The Journal of Physical Chemistry Letters. 7 (2016) 5291–5296. doi:10.1021/acs.jpclett.6b02090.